

On the Observability of Collective Flavor Oscillations in Diffuse Supernova Neutrino Background

Sovan Chakraborty,¹ Sandhya Choubey,² and Kamales Kar¹

¹*Saha Institute of Nuclear Physics, 1/AF Bidhannagar, Kolkata 700064, India*

²*Harish-Chandra Research Institute, Chhatnag Road, Jhansi, Allahabad 211019 India*

Collective flavor oscillations are known to bring multiple splits in the supernova (SN) neutrino and antineutrino spectra. These spectral splits depend not only on the mass hierarchy of the neutrinos but also on the initial relative flux composition. Observation of spectral splits in a future galactic supernova signal is expected to throw light on the mass hierarchy pattern of the neutrinos. However, since the Diffuse Supernova Neutrino Background (DSNB) comprises of a superposition of neutrino fluxes from all past supernovae, and since different supernovae are expected to have slightly different initial fluxes, it is pertinent to check if the hierarchy dependent signature of collective oscillations can survive this averaging of the flux spectra. Since the actual distribution of SN with initial relative flux spectra of the neutrinos and antineutrinos is unknown, we assume a log-normal distribution for them. We study the dependence of the hierarchy sensitivity to the mean and variance of the log-normal distribution function. We find that the hierarchy sensitivity depends crucially on the mean value of the relative initial luminosity. The effect of the width is to reduce the hierarchy sensitivity for all values of the mean initial relative luminosity. We find that in the very small mixing angle (θ_{13}) limit considering only statistical errors even for very moderate values of variance, there is almost no detectable hierarchy sensitivity if the mean relative luminosities of ν_e and $\bar{\nu}_e$ are greater than 1.

I. INTRODUCTION

Neutrinos coming from supernova explosions can give rich information about the explosion mechanism as they are the only particles that come from regions deep inside the core. They are also extremely useful for determining neutrino properties as neutrinos from SN1987A have amply demonstrated [1–3]. In particular, it has been shown that the neutrino mass hierarchy and smallness of θ_{13} can be probed using SN neutrinos [4, 5]. In the last few years, focus has been on the effect of neutrino-neutrino interaction in the central regions of the core of supernova, giving rise to the so-called collective effects [6–43].

The ‘collective’ nature of simultaneous flavor conversions of both neutrinos and antineutrinos give rise to ‘splits’ in the spectra of the neutrinos and antineutrinos. These splits occur due to sudden change in the oscillation probability, causing spectral swaps which may end up in observable effects. Interestingly the impact of collective oscillations on the spectra are different for the Normal Hierarchy (NH) and the Inverted Hierarchy (IH). This opens up the possibility of identifying the neutrino mass hierarchy via observation of collective effects in the neutrino signal from a future galactic supernova event [30].

However with the very small rate of occurrence of galactic supernova events (a few per century) one is forced to think of strategies of detecting the above mentioned effect otherwise. One of the promising possibilities is the detection of Diffuse Supernova Neutrino Background (DSNB) in the near future [44–46]. The cumulative number of neutrinos and antineutrinos produced by all earlier SN events in the universe result in a cosmic background known as DSNB. Though these neutrinos are yet to be detected, one has reasons to believe that it may be possible to observe them in the near future [47–66].

Present day upper limits are $1.2 \bar{\nu}_e \text{ cm}^{-2} \text{ s}^{-1}$ with energies above 19.3 MeV for Super-Kamiokande (SK) water Cerenkov detectors [67]) and $6.8 \times 10^3 \text{ cm}^{-2} \text{ s}^{-1}$ with energies between 25 MeV and 50 MeV for Liquid Scintillator Detector (LSD) [68] at 90% C.L. for both.

The two key ingredients in the calculation of DSNB are (i) the SN rate which is proportional to cosmic star formation rate and (ii) the ν and $\bar{\nu}$ energy spectra. Whereas reliable estimates are now available for the star formation rate and the SN rate [69, 70], the prediction for the SN neutrino spectra has gone through an evolution over the years. Earlier considerations of matter induced resonances were followed by incorporating the ‘collective’ effects due to interaction amongst the neutrinos themselves in the high density central regions of the core. The first study of the effect of the collective flavor oscillations on DSNB fluxes and the corresponding predicted number of events in terrestrial detectors were carried out in [65] where it was demonstrated that the event rate gets substantially modified by collective effects. The results also showed that observation of the DSNB fluxes at earth could shed light on the neutrino mass hierarchy. However, since then substantial progress has been made in the understanding of the collective effects. In particular, it is now clear that the neutrino and antineutrino survival probability and hence different split patterns depend crucially on the relative luminosities of the initial neutrino fluxes produced inside the exploding star [36–38]. Therefore, one can predict the final neutrino and antineutrino spectra from a given SN with reasonable accuracy only if one already has access to the initial flux conditions. This complication is further compounded for the DSNB, as the DSNB flux comes from a superposition of the fluxes from all past SNe. Since the initial flux conditions are expected to be sensitive to the properties of the progen-

itor star and since we have a whole distribution of stars which end up being a SN, it is a complicated business to accurately estimate the DSNB spectra after accounting for the collective effects, which are bound to happen in almost every SN.

In this work we incorporate the observation of different split patterns in the spectra for the calculation of DSNB and do not take the relative (anti)neutrino fluxes to have fixed values. The main focus of this work is to check the effect of a distribution of supernovae with initial flux on the measurement of the neutrino mass hierarchy via the observation of the DSNB signal. Since the distribution of the initial fluxes over all past SNe are not available to us, we parametrize this by a log-normal distribution. The log-normal distribution has two parameters which define the mean and width of the distribution. Since they are also unknown, we choose various plausible values for them. We calculate the DSNB event rate averaged over these distributions. We study how the hierarchy measurement is affected when one takes the distribution of initial relative fluxes into account and find situations where the hierarchy determination may be possible.

II. THE DIFFUSE SUPERNOVA NEUTRINO BACKGROUND

The differential number flux of DSNB is

$$F'_\nu(E_\nu) = \frac{c}{H_0} \int_0^{z_{max}} R_{SN}(z) F_\nu(E) \frac{dz}{\sqrt{\Omega_m(1+z)^3 + \Omega_\Lambda}} \quad (1)$$

where $E_\nu = (1+z)^{-1}E$ is the redshifted neutrino energy observed at earth while E is the neutrino energy produced at the source, F_ν is the neutrino flux for each core collapse SN, $R_{SN}(z)$ the cosmic SN rate at redshift z , and the Hubble constant taken as $H_0 = 70 h_{70} \text{ km s}^{-1} \text{ Mpc}^{-1}$. For the standard Λ -CDM cosmology, we have matter and dark energy density $\Omega_m = 0.27$ and $\Omega_\Lambda = 0.73$, respectively [71]. As Eq. (1) suggests the DSNB flux at earth depends on two factors: (i) the cosmic SN rate and (ii) the initial SN neutrino spectrum from each SN.

The cosmic SN rate is related to the star formation rate $R_{SF}(z)$, through a suitable choice of Initial Mass Function (IMF) as $R_{SN}(z) = 0.0132 \times R_{SF}(z) M_\odot^{-1}$ [72, 73]. The IMF takes into account that only stars with masses larger than $8M_\odot$ result in supernova explosion. For the cosmic star formation rate per co-moving volume we take

$$R_{SF}(z) = 0.32 f_{SN} h_{70} \frac{e^{3.4z}}{e^{3.8z} + 45} \frac{\sqrt{\Omega_m(1+z)^3 + \Omega_\Lambda}}{(1+z)^{3/2}} \quad (2)$$

where f_{SN} is normalization of the order of unity and $R_{SF}(z)$ is in units of $M_\odot \text{ yr}^{-1} \text{ Mpc}^{-3}$ [54, 74]. The initial SN neutrino spectrum emitted from the neutrinosphere

is parametrized in the form [75]

$$\begin{aligned} F_\nu^0(E) &= \left(\frac{L_\nu^0}{E}\right) \times \left(\frac{(1+\alpha)^{1+\alpha}}{\Gamma(1+\alpha)\bar{E}}\right) \left(\frac{E}{\bar{E}}\right)^\alpha e^{-(1+\alpha)E/\bar{E}} \\ &= \phi_\nu^0 \times \psi(E), \end{aligned} \quad (3)$$

where ϕ_ν^0 is the total initial flux estimated for the initial luminosity L_ν^0 and average energy \bar{E} . The spectral shape also depends on the energy distribution $\psi(E)$, which is parametrized by the pinching parameter α . In this study we use $\bar{E}_{\nu_e} = 12 \text{ MeV}$, $\bar{E}_{\bar{\nu}_e} = 15 \text{ MeV}$, $\bar{E}_{\nu_x} = \bar{E}_{\nu_y} = 18 \text{ MeV}$ with $\alpha_{\nu_x} = \alpha_{\bar{\nu}_x} = \alpha_{\nu_y} = \alpha_{\bar{\nu}_y} = 4$ and $\alpha_{\nu_e} = \alpha_{\bar{\nu}_e} = 3$. Here ν_x is a linear combination of ν_μ, ν_τ and ν_y is the combination orthogonal to ν_x ; in our case ν_x and ν_y has same flux hence $F_{\nu_x} = F_{\nu_y}$. The average energies of the different flux types will also vary from SN to SN. However for simplicity, in this work we choose to keep the average energies fixed. We assume that 3×10^{53} erg of energy is released in (anti)neutrinos by all SNe.

The emitted spectrum $F_\nu(E)$ is processed by collective flavor oscillation and MSW oscillation effects over the huge drop of matter density inside SN. The collective oscillations are over within a few 100 km from neutrinosphere whereas the MSW oscillation takes place in the region $10^4 - 10^5 \text{ km}$ [76] for the solar and atmospheric mass squared differences. As the collective and MSW oscillations are widely separated in space, they can be considered independent of each other [35]. Thus the flux reaching the MSW resonance region already has the effects of the collective oscillations. This assumption may not hold in SN models [15], where at late times the MSW resonance and the collective effects can be simultaneous as there the matter density falls substantially compared to the early time. In the time integrated DSNB flux it can give rise to some corrections. However we have ignored these effects as in this work we followed matter profile from studies [35] with larger matter density [76, 77] finding the two oscillations regimes to be mutually exclusive even at late times.

It has been seen that collective oscillations can give rise to different split patterns of the neutrino spectra depending on the initial relative flux of ν_e and $\bar{\nu}_e$ with respect to flavor ν_x or ν_y , so we define $\phi_{\nu_e}^r = \frac{\phi_{\nu_e}^0}{\phi_{\nu_x}^0}$ and $\phi_{\bar{\nu}_e}^r = \frac{\phi_{\bar{\nu}_e}^0}{\phi_{\nu_x}^0}$ as measures of the relative fluxes [38]. The electron antineutrino flux beyond the collective region can swap to x flavor above some energy (single split) or can swap in some energy interval (double split) or even can remain unchanged (no split) depending on the initial relative flux $\phi_{\nu_e}^r$ and $\phi_{\bar{\nu}_e}^r$ [36–38]. DSNB is affected differently with these different oscillation scenarios. To incorporate the effect of collective oscillations we work in a effective two flavor scenario with single angle approximation¹.

¹ Multi-angle effects can give rise to kinematical decoherence among angular modes and smear the spectral splits [17], how-

Recent papers [39, 42] have explored the effect of three flavors on the outcome of the split patterns in collective oscillations. The three flavor results differ a bit from the two flavors only for IH and that too in a small region of the initial flux parameter space $(\phi_{\nu_e}^r, \phi_{\bar{\nu}_e}^r)$, where single split (in 3 flavor) appears instead of the double splits (in 2 flavor). However the observed single split in NH for this region remains unchanged in the 3 flavor treatment [42]. Thus in a small part [37, 38] of the parameter space $(\phi_{\nu_e}^r, \phi_{\bar{\nu}_e}^r)$, where 2 and 3 flavor results differ, both IH and NH have similar split pattern (single split) for the 3 flavor evolution. In other parts of the initial flux parameter space the split patterns remain the same. Therefore while averaging over the whole parameter space the corrections in the 3 flavor treatment compared to the 2 flavor one coming from the small region would not be appreciable. The main conclusions of this paper – as we later see – therefore remain largely independent of these small corrections. Moreover the three flavor effects are also found to be sensitive to the neutrino-neutrino interaction potential, the evolution of a three flavor system effectively behaves like a two flavor one with the reduction of the neutrino-neutrino interaction potential by only one order [42]. Hence for such a smaller neutrino-neutrino potential the two flavor treatment of the collective evolution is reasonable and for larger values the two flavor treatment can be again be considered as a reasonable approximation when averaging over the whole initial flux parameter space is taken into account.

In this effective two flavor treatment the collective oscillations involve only two flavors (ν_e, ν_x) , while the other flavor (ν_y) does not evolve. Thus the Flux $(F_{\nu_\alpha}^c)$ after the collective oscillations are given by

$$F_{\nu_e}^c = P_c F_{\nu_e}^0 + (1 - P_c) F_{\nu_x}^0, \quad F_{\bar{\nu}_e}^c = \bar{P}_c F_{\bar{\nu}_e}^0 + (1 - \bar{P}_c) F_{\bar{\nu}_x}^0.$$

Similarly the quantities $F_{\nu_x}^c$ and $F_{\bar{\nu}_x}^c$ can be estimated from the relations

$$F_{\nu_x}^c + F_{\nu_e}^c = F_{\nu_e}^0 + F_{\nu_x}^0 \quad \text{and} \quad F_{\bar{\nu}_x}^c + F_{\bar{\nu}_e}^c = F_{\bar{\nu}_e}^0 + F_{\bar{\nu}_x}^0.$$

As for the other flavor ν_y ($\bar{\nu}_y$) there is no collective evolution, hence $F_{\nu_y}^c = F_{\nu_y}^0$ ($F_{\bar{\nu}_y}^c = F_{\bar{\nu}_y}^0$). The quantities P_c and \bar{P}_c are the neutrino and antineutrino survival probability after the collective effect, respectively. The only way ν_y can affect the final neutrino spectrum is by MSW transition. As we consider self-induced neutrino oscillations to happen independent of the MSW, so the pre-processed flux $F_{\nu_\alpha}^c$ and the unchanged ‘y’ flavor will undergo the traditional MSW conversions.

In NH the MSW resonances affect the ν_e flux, while the $\bar{\nu}_e$ flux remains almost unaffected. However for IH, MSW affect the $\bar{\nu}_e$ flux, and not the ν_e flux. Then these neutrinos get redshifted while traveling independently as

ever for spherical symmetry the single angle approximation i.e. neutrino-neutrino interactions averaged along a single trajectory comes out to be a fine approximation as the multi angle decoherence in such a case is weak against the collective features [18, 36, 78]

Normal hierarchy
$F_{\nu_e} = s_{12}^2 P_c (\phi_{\nu_e}^r, \phi_{\bar{\nu}_e}^r, E) (2P_H - 1) (F_{\nu_e}^0 - F_{\nu_x}^0) + s_{12}^2 (1 - P_H) (F_{\nu_e}^0 - F_{\nu_x}^0) + F_{\nu_x}^0.$
$F_{\bar{\nu}_e} = c_{12}^2 \bar{P}_c (\phi_{\nu_e}^r, \phi_{\bar{\nu}_e}^r, E) (F_{\bar{\nu}_e}^0 - F_{\nu_x}^0) + F_{\nu_x}^0.$
Inverted hierarchy
$F_{\nu_e} = s_{12}^2 P_c (\phi_{\nu_e}^r, \phi_{\bar{\nu}_e}^r, E) (F_{\nu_e}^0 - F_{\nu_x}^0) + F_{\nu_x}^0.$
$F_{\bar{\nu}_e} = c_{12}^2 \bar{P}_c (\phi_{\nu_e}^r, \phi_{\bar{\nu}_e}^r, E) (2P_H - 1) (F_{\bar{\nu}_e}^0 - F_{\nu_x}^0) + c_{12}^2 (1 - P_H) (F_{\bar{\nu}_e}^0 - F_{\nu_x}^0) + F_{\nu_x}^0.$

TABLE I: Electron neutrino and antineutrino spectra emerging from a SN.

mass-eigenstates until they reach earth, here they are detected as flavor eigenstates before or after having undergone regeneration inside the earth. The fluxes $(F_{\nu_e}$ and $F_{\bar{\nu}_e})$ arriving at earth after both the collective and MSW oscillation are given in Table I.

In Table I, P_H is the effective jump probability between the neutrino mass eigenstates due to the atmospheric mass squared driven MSW resonance. It takes a value between 0 and 1 depending on the value of the mixing angle θ_{13} . For θ_{13} large ($\sin^2 \theta_{13} \gtrsim 0.01$) $P_H \simeq 0$, while for small θ_{13} ($\sin^2 \theta_{13} \lesssim 10^{-6}$) $P_H \simeq 1$ [79]. For the smaller limit of θ_{13} the effective jump probability has a non-trivial dependence on energy and time, due to multiple resonances [14, 19] and turbulence [16, 17, 18]. Since these effects occur in the small time-window when the shock wave is in the resonance region one can neglect this sub-leading effect in the time integrated observables like DSNB events. The quantities s_{12}^2 and c_{12}^2 stand for $\sin^2 \theta_{12}$ (taken to be 0.3 for numerical studies) and $\cos^2 \theta_{12}$, respectively. The neutrino and antineutrino survival probability after the collective effect are calculated numerically taking $\Delta m^2 = 3 \times 10^{-3} \text{ eV}^2$ and a small effective mixing angle of 10^{-5} . However it should be noted that the collective probabilities P_c and \bar{P}_c are almost independent of the specific non zero values of the mixing angle [16, 23, 36]. Thus the effective mixing angle in the matter for both the limits $\sin^2 \theta_{13} \gtrsim 0.01$ and $\sin^2 \theta_{13} \lesssim 10^{-6}$ will give rise to similar collective features. We checked explicitly that the results remain the same when one varies the effective mixing angle by orders of magnitude. Hence for the collective evolutions we consider a representative value of 10^{-5} as the effective mixing angle for both the limits. For further details of analysis of the collective effects we refer the reader to [38].² As discussed before, P_c and/or \bar{P}_c , which is a function of the neutrino energy E , show pattern of sudden change between 0 and 1, leading to sudden change in the neutrino and/or antineutrino spectra. Depending on

² Note that $P_c = \bar{P}_c = 1$ gives back the SN flux without collective oscillation [4]

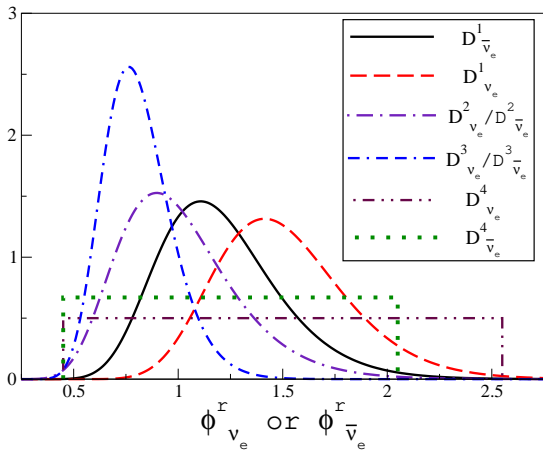


FIG. 1: The four specimen distributions used in the calculations. The y-axis gives the distribution of supernova in arbitrary units.

the number of times the value of P_c (and/or \bar{P}_c) changes, we can have more than one sudden swap of the neutrino (and/or antineutrino) spectra, referred to in the literature as multiple split [36–38]. The split patterns are now known to be crucially dependent on the initial relative flux densities of the neutrino and antineutrino. The initial relative neutrino and antineutrino flux densities are expected to vary among different SN.

This variation in $\phi_{\nu_e}^r$ and $\phi_{\bar{\nu}_e}^r$ in different SNe might have origin in difference of progenitor mass, different luminosity etc. In fact even different simulations allow wide variation of $\phi_{\nu_e}^r$ and $\phi_{\bar{\nu}_e}^r$ within the 2 fold uncertainty around equipartition ($\frac{\bar{E}_{\nu_e}}{2E_{\nu_e}} \leq \phi_{\nu_e}^r \leq \frac{2\bar{E}_{\nu_e}}{E_{\nu_e}}; \frac{\bar{E}_{\bar{\nu}_e}}{2E_{\bar{\nu}_e}} \leq \phi_{\bar{\nu}_e}^r \leq \frac{2\bar{E}_{\bar{\nu}_e}}{E_{\bar{\nu}_e}}$) [5]. Most models predict $l_{\nu_e} \simeq l_{\bar{\nu}_e}$, where l_{ν_e} and $l_{\bar{\nu}_e}$ are the relative luminosity ($\frac{L_{\nu_e}}{L_{\tau_{total}}}$) of ν_e and $\bar{\nu}_e$ respectively [37]. However, the combined luminosity of $\nu_\mu, \nu_\tau, \bar{\nu}_\mu$ and $\bar{\nu}_\tau$ is seen to be rather disparate between the different model results³. The most reliable way to reconstruct the relative luminosity distribution function in principle would be from direct observation of SN events along with their neutrino signal. However, as yet only SN1987A has been observed along with the detection of its neutrinos/antineutrinos. We require to know neutrino fluxes of different flavors from a number of galactic SN with a range of stellar mass and initial conditions before collapse to have information about the possible variation in $\phi_{\nu_e}^r$ and $\phi_{\bar{\nu}_e}^r$. This might take decades and is clearly not possible in the near future. So we propose in this paper that the SN events contributing to DSNB have various different values of $\phi_{\nu_e}^r$ and $\phi_{\bar{\nu}_e}^r$. For quantitative estimates we assume specific distributions for them. We

take $\phi_{\nu_e}^r$ and $\phi_{\bar{\nu}_e}^r$ distributed log-normally, defined by the parameters (μ_1, σ_1) and (μ_2, σ_2) i.e,

$$D_\nu(\mu_1, \sigma_1) = \frac{e^{-\left(\frac{\log(\phi_{\nu_e}^r) - \mu_1}{2\pi\sigma_1}\right)^2}}{\sqrt{2\pi}\sigma_1\phi_{\nu_e}^r};$$

$$D_{\bar{\nu}}(\mu_2, \sigma_2) = \frac{e^{-\left(\frac{\log(\phi_{\bar{\nu}_e}^r) - \mu_2}{2\pi\sigma_2}\right)^2}}{\sqrt{2\pi}\sigma_2\phi_{\bar{\nu}_e}^r}. \quad (4)$$

We choose a range of values for μ such that the expectation (mean) values of $\phi_{\nu_e}^r$ and $\phi_{\bar{\nu}_e}^r$ are compatible with either Lawrence Livermore (equipartition) or Garching simulations. The parameter σ determines the width of the distribution. Since the variation of $\phi_{\nu_e}^r$ and $\phi_{\bar{\nu}_e}^r$ is expected to be within the 2 fold uncertainty around equipartition [5], the σ 's for the distributions are chosen such that the distribution is well within the 2 fold uncertainty of the expectation value. In order to show the effect of the choice of the distribution function we simulate our results for four widely different distributions for $\phi_{\nu_e}^r$ and $\phi_{\bar{\nu}_e}^r$. They are chosen as follows:

1. The expectation is the equipartition value, i.e 1.5 for $\phi_{\nu_e}^r$ and 1.2 for $\phi_{\bar{\nu}_e}^r$ and the variation is within 2 fold uncertainty of 1.5 and 1.2 respectively. The corresponding values of (μ, σ) turn out to be (0.39, 0.21) for neutrinos and (0.16, 0.24) for antineutrinos. We denote this distributions by $D_{\nu_e}^1$ and $D_{\bar{\nu}_e}^1$.
2. The expectation is same for both $\phi_{\nu_e}^r$ and $\phi_{\bar{\nu}_e}^r$ and is taken as 1, the σ is chosen as stated above. Hence the distributions for ν_e and $\bar{\nu}_e$ are identical and is defined by the parameters $(\mu, \sigma) \equiv (-0.03, 0.28)$. We denote this distribution by $D_{\nu_e}^2$ and $D_{\bar{\nu}_e}^2$.
3. The expectation is taken to be the same as the Garching simulations [75], i.e 0.8 for both the ν_e and $\bar{\nu}_e$ and the distributions parametrized by $(\mu, \sigma) \equiv (-0.23, 0.20)$ are the same. We denote this distribution by $D_{\nu_e}^3$ and $D_{\bar{\nu}_e}^3$.
4. We consider the distribution to be constant between 0.45-2.55 for $\phi_{\nu_e}^r$ and 0.45-2.05 for $\phi_{\bar{\nu}_e}^r$, with a normalization factor of $\frac{1}{2.1}$ and $\frac{1}{1.6}$ respectively. We denote this case by $D_{\nu_e}^4$ and $D_{\bar{\nu}_e}^4$.

The four specimen distributions for $\phi_{\nu_e}^r$ and $\phi_{\bar{\nu}_e}^r$ are shown in Fig. 1. By definition the log-normal distribution functions D^1, D^2 and D^3 are normalized to unity. The choice of our normalization factors for the uniform distribution functions in D^4 ensures that they are normalized to unity as well. We can see from the figure that D^3 has the narrowest spread in the relative flux while the uniform distribution D^4 has the widest. For simplicity we have chosen distribution functions that are independent of the redshift z .

³ See for e.g. the compilation of model results in [80].

The differential number flux of DSNB with the i^{th} distributions is given by

$$F_{\nu}^i(E_{\nu}) = \frac{c}{H_0} \int_{\phi_{\nu_e}^{\text{min}}^r}^{\phi_{\nu_e}^{\text{max}}^r} \int_{\phi_{\bar{\nu}_e}^{\text{min}}^r}^{\phi_{\bar{\nu}_e}^{\text{max}}^r} \int_0^{z_{\text{max}}} R_{SN}(z) F_{\nu}(E, \phi_{\nu_e}^r, \phi_{\bar{\nu}_e}^r) \times D_{\nu_e}^i(\phi_{\nu_e}^r) D_{\bar{\nu}_e}^i(\phi_{\bar{\nu}_e}^r) \frac{dz d\phi_{\nu_e}^r d\phi_{\bar{\nu}_e}^r}{\sqrt{\Omega_m(1+z)^3 + \Omega_{\Lambda}}}, \quad (5)$$

where $D_{\nu_e}^i(\phi_{\nu_e}^r)$ and $D_{\bar{\nu}_e}^i(\phi_{\bar{\nu}_e}^r)$ is the number of supernovae in between the interval $\phi_{\nu_e}^r$ to $\phi_{\nu_e}^r + d\phi_{\nu_e}^r$ and $\phi_{\bar{\nu}_e}^r$ to $\phi_{\bar{\nu}_e}^r + d\phi_{\bar{\nu}_e}^r$, respectively. $F_{\nu}(E, \phi_{\nu_e}^r, \phi_{\bar{\nu}_e}^r)$ is the neutrino flux of each SN with initial relative flux combination $\phi_{\nu_e}^r$ and $\phi_{\bar{\nu}_e}^r$ at a redshift z . z_{max} is taken as 5, where as $\phi_{\alpha\text{min}}^r$ and $\phi_{\alpha\text{max}}^r$ are chosen from the 2 fold uncertainty around expectation of the respective distribution. The upper panel in Fig. 2 shows the antineutrino DSNB flux (in logarithmic scale) for NH and the lower panel shows the flux for IH with $P_H=1$. In both panels flux is shown for all of our different distribution (D^1 - D^4) of $\phi_{\nu_e}^r$ and $\phi_{\bar{\nu}_e}^r$. In Fig. 2 we also plotted flux for the case without any distribution of $\phi_{\nu_e}^r$ and $\phi_{\bar{\nu}_e}^r$ but specific value (0.8, 0.8) for the initial relative fluxes ($\phi_{\nu_e}^r, \phi_{\bar{\nu}_e}^r$). From the

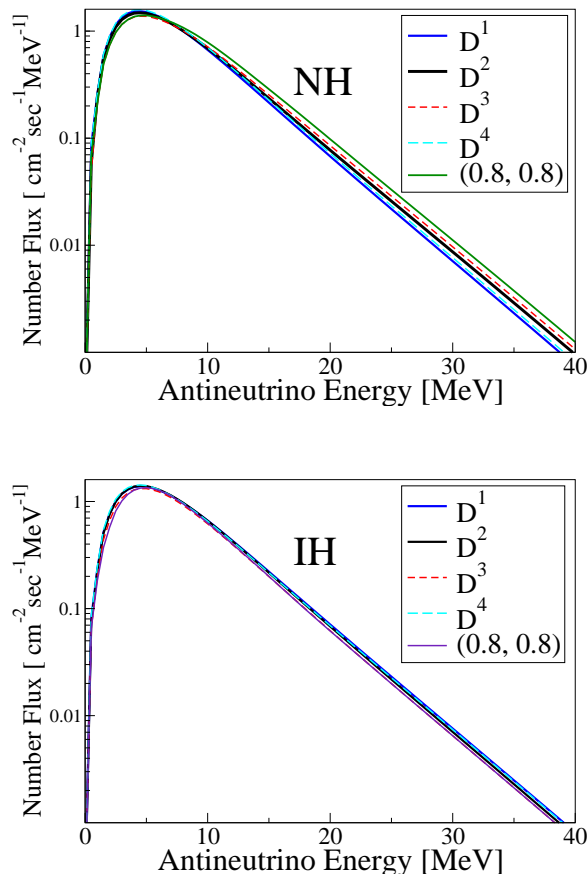


FIG. 2: $\bar{\nu}_e$ fluxes for NH(upper panel) and IH (lower panel) with small θ_{13} , i.e $P_H=1$.

Model	Hierarchy	2.5 Mton-yr (19.3 - 30.0) (MeV)	GD+2.5 Mton-yr (10.0 - 30.0) (MeV)
D^1	NH	76±9	280±17
	IH ($P_H=0$)	92±10	319±18
	IH ($P_H=1$)	80±9	288±17
(1.5, 1.2)	NH	75±9	281±17
	IH ($P_H=0$)	98±10	332±19
	IH ($P_H=1$)	75±9	280±17
D^2	NH	88±10	307±18
	IH ($P_H=0$)	103±11	350±19
	IH ($P_H=1$)	76±9	280±17
(1.0, 1.0)	NH	102±11	340±19
	IH ($P_H=0$)	103±11	341±19
	IH ($P_H=1$)	77±9	295±18
D^3	NH	98±10	334±19
	IH ($P_H=0$)	113±11	379±20
	IH ($P_H=1$)	70±9	258±16
(0.8, 0.8)	NH	112±11	378±20
	IH ($P_H=0$)	113±11	378±20
	IH ($P_H=1$)	70±9	260±17
D^4	NH	82±9	297±18
	IH ($P_H=0$)	97±10	335±19
	IH ($P_H=1$)	79±9	283±17
(1.5, 1.25)	NH	77±9	286±18
	IH ($P_H=0$)	97±10	330±19
	IH ($P_H=1$)	76±9	285±17

TABLE II: Number of expected events per 2.5 Megaton-year of a water Cherenkov with SK like resolution and in a similar detector with Gadolinium loaded.

flux figures it is evident that the different distributions give similar DSNB flux. To check whether the small differences in their profile are measurable or not we next calculate the corresponding event rate in different detectors.

III. DSNB EVENT RATES AND HIERARCHY MEASUREMENT

Since the DSNB fluxes are very small, they are expected to be observed in either very large detectors or in reasonable size detectors with very large exposure times. The only reasonable size detector running currently is the Super-Kamiokande (SK) [67]. Amongst the proposed large detectors which have low energy threshold are the megaton water Cherenkov detectors [81–83], Gadolinium enriched water Cherenkov detectors [84] (which could be SK or possibly an even larger water detector), very large liquid scintillator detector (LENA) [53] or very large liquid Argon detector [85–87]. Apart from the liquid Argon detector, none of the other detectors hold much promise

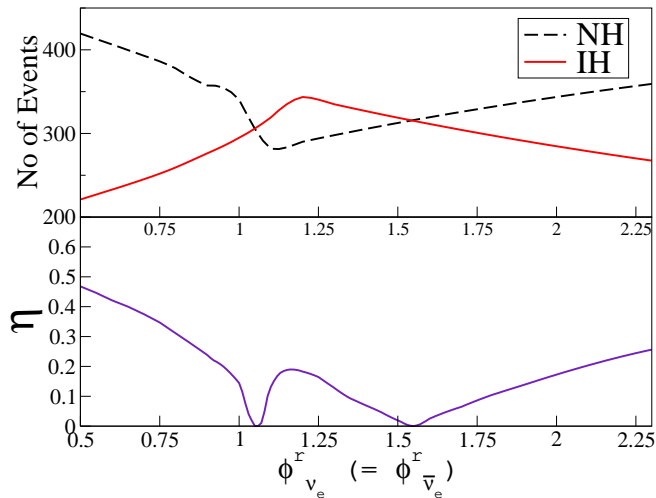


FIG. 3: Upper panel shows the number of expected DSNB events in 2.5 MtonYr of Gadolinium loaded water detector for normal (NH) and inverted (IH) hierarchies (for IH, $P_H = 1$) as a function of $\phi_{\nu_e}^r (= \phi_{\bar{\nu}_e}^r)$. The lower panel shows the change of η as a function of $\phi_{\nu_e}^r (= \phi_{\bar{\nu}_e}^r)$.

for the detection of DSNB ν_e . Therefore, in rest of this discussion we will focus only on the detection possibilities for the DSNB $\bar{\nu}_e$ fluxes. All detector technologies mentioned above use the inverse beta decay $\bar{\nu}_e + p \rightarrow n + e^+$ interaction for detecting DSNB fluxes. The only difference between them would be in terms of their energy window of sensitivity for the DSNB. Water detectors use the neutrino energy (E_ν) window 19.3 MeV to 30.0 MeV [67], whereas for Gadolinium loaded water detectors the detection window is between 10 MeV and 30 MeV [84]. Liquid scintillator on the other hand has a sensitivity range between 10 MeV and 25 MeV [53]. We show the total number of events for 2.5 Mton-yr exposure in water detectors and 2.5 Mton-yr exposure in Gadolinium loaded water detectors in the third and fourth columns of Table II. The number of events are shown for the four different specimen distributions. Results are shown separately for $P_H = 1$ and $P_H = 0$ when the neutrino mass hierarchy is inverted (IH). For the NH, there is no dependence of the $\bar{\nu}_e$ flux on P_H , as one can see from Table I. In each case we also show for comparison the number of events expected when $\phi_{\nu_e}^r$ and $\phi_{\bar{\nu}_e}^r$ are fixed at their respective mean values of the distribution⁴. Observing a variation of the number of events changing the $\phi_{\nu_e}^r$ and $\phi_{\bar{\nu}_e}^r$ for these examples without any distribution is an important indicator of how inclusion of distribution can change the DSNB event numbers.

We next turn our attention to the possibility of measuring the neutrino mass hierarchy using DSNB detec-

tion. For the distribution examples D^1 , D^2 and D^4 the difference of number of events between NH and IH (both $P_H = 1$ and $P_H = 0$) seems to be within statistical uncertainty. Whereas for the distribution D^3 , though the difference in number of events between NH and IH (with $P_H = 1$) decreases significantly compared to the without distribution case, the difference is still greater than the statistical uncertainty. To probe this variation of hierarchy sensitivity with the distribution further let us define the quantity

$$\eta = \frac{|N_{NH} - N_{IH}|}{N_{NH}}, \quad (6)$$

which gives a measure of the hierarchy sensitivity of the experiment. The quantities N_{NH} and N_{IH} are the number of expected DSNB events when the hierarchy is normal and inverted, respectively. The quantity η is definitely not an observable as it depends on both N_{NH} and N_{IH} . However it helps describing the variation of hierarchy sensitivity of DSNB in a systematic manner. There are two ingredients of interest in Table II. Firstly, we can see that the relative hierarchy difference η depends on the mean value of $\phi_{\nu_e}^r$ and $\phi_{\bar{\nu}_e}^r$. Secondly, for a given $\langle \phi_{\nu_e}^r \rangle$ and $\langle \phi_{\bar{\nu}_e}^r \rangle$ it also depends on the distribution function involved.

For a better understanding of the first issue, we show in the upper panel of Fig. 3 the variation of the number of events for both the NH and IH cases, as a function of the relative luminosity factor. The analysis is again done for the small mixing angle limit ($P_H = 1$) for IH, as it is the more challenging limit from the experimental point of view. We show this for 2.5 MegatonYears of Gadolinium doped water detector⁵. For simplicity we have taken $\phi_{\nu_e}^r = \phi_{\bar{\nu}_e}^r$ in this figure and we do not take any distribution function into account. The lower panel shows the corresponding η as a function of $\phi_{\nu_e}^r = \phi_{\bar{\nu}_e}^r$. We see that η has a very complicated dependence on the relative initial luminosity functions. The variation of η with $\phi_{\nu_e}^r$ actually depends on several factors like difference between split pattern of NH and IH, the split/swap energies, the initial relative flux of ν_e , $\bar{\nu}_e$ and ν_x . It is rather high for very low values of $\phi_{\nu_e}^r$ and $\phi_{\bar{\nu}_e}^r$. It starts decreasing as the value of $\phi_{\nu_e}^r$ and $\phi_{\bar{\nu}_e}^r$ increase until it becomes zero around $\phi_{\nu_e}^r = \phi_{\bar{\nu}_e}^r \simeq 1.05$, thereafter it increases for a short while until it reaches a (local) maximum at around $\phi_{\nu_e}^r = \phi_{\bar{\nu}_e}^r \simeq 1.25$. Beyond that the value of η decreases again reaching a second zero at around $\phi_{\nu_e}^r = \phi_{\bar{\nu}_e}^r \simeq 1.5$. After that it increases monotonically.

The most noteworthy thing in the upper panel of this figure is that the number of events for inverted hierarchy

⁴ For the uniform distribution D^4 we took the central values of the widths as their representative mean.

⁵ Most of the results shown in this paper is for megaton class Gadolinium doped water detector to show the impact of the relative initial luminosity and its distribution on the hierarchy measurement using DSNB fluxes. The corresponding sensitivities for smaller scale detectors can be calculated trivially using these numbers.

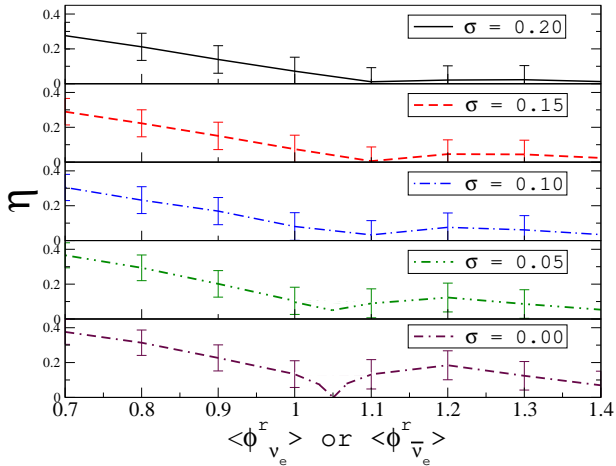


FIG. 4: Relative difference (η) of number of expected events in normal and inverted hierarchy, per 2.5 Megaton-year in a Gadolinium loaded SK like detector. For the IH case we consider small mixing angle i.e $P_H = 1$. The above panels show η for four possible cases with σ being 0.00, 0.05, 0.10, 0.15 and 0.20. The x axis denotes the expectation of $\phi_{\nu_e}^r$ and $\phi_{\bar{\nu}_e}^r$ for the chosen sigma. Here expectation of $\phi_{\nu_e}^r$ and $\phi_{\bar{\nu}_e}^r$ are taken to be same i.e $\mu_1 = \mu_2$. The errors shown are the statistical errors only.

has almost linear dependence on $\phi_{\nu_e}^r = \phi_{\bar{\nu}_e}^r$ on both sides of the maximum which comes around $\phi_{\nu_e}^r = \phi_{\bar{\nu}_e}^r \simeq 1.25$. For the normal hierarchy one sees departure from linearity around $\phi_{\nu_e}^r = \phi_{\bar{\nu}_e}^r \simeq 1.1$. This feature is crucial in determining the effect of the distribution function on the hierarchy sensitivity. The effect of taking the distribution function into account boils down to creating a weighted average of the number of events, where the weights are determined by the distribution itself. For the log-normal case the weights are driven by the mean and width of the distribution, which we parametrize in terms of μ and σ . The effect of any distribution can thus be understood with the help of Fig. 3.

To show the effect of the distribution function we continue to stick to the simplified scenario where $\phi_{\nu_e}^r = \phi_{\bar{\nu}_e}^r$ and show in Fig. 4 the relative difference η as a function of the expectation value $\langle \phi_{\nu_e}^r \rangle (= \langle \phi_{\bar{\nu}_e}^r \rangle)$. Here again we take $P_H = 1$ for IH. We consider log-normal distribution for the relative luminosities⁶ and show η for five different values of σ which controls the width of the distribution. The values and error bars on η correspond to a statistics of 2.5 Megaton-Year data in Gadolinium loaded water detector. The lowest panel with $\sigma = 0$ corresponds to the case where we keep $\phi_{\nu_e}^r$ ($\phi_{\bar{\nu}_e}^r$) fixed and for this case there is no effect of the distribution. This case is similar

⁶ Our conclusions remain fairly robust against the choice of the distribution function. We have explicitly checked this by repeating Fig. 4 with uniform distribution and normal distribution. However, we do not present those results as they follow the same pattern that we get for the log-normal distribution.

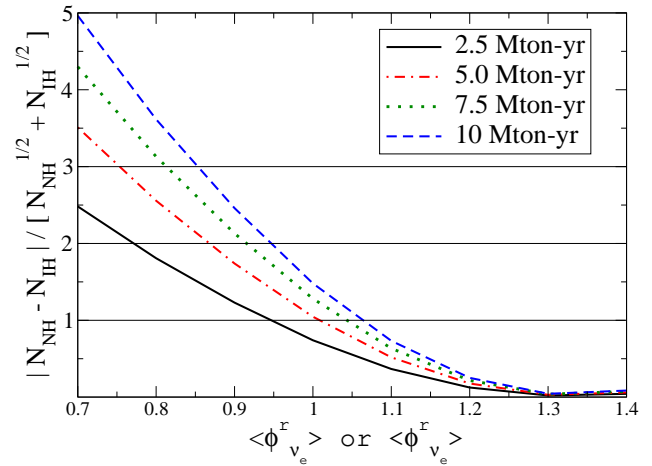


FIG. 5: Plot of $\frac{|N_{NH} - N_{IH}|}{\sqrt{N_{NH} + N_{IH}}}$ with $\langle \phi_{\nu_e}^r \rangle (= \langle \phi_{\bar{\nu}_e}^r \rangle)$ for $\sigma=0.20$. The ratio is shown for a Gadolinium loaded SK like detector with different values of the exposure i.e. 2.5, 5.0, 7.5 and 10.0 Mton-Yr. Horizontal line at ratio 1 denotes that statistical error is of the same order as the difference between two hierarchies. Higher values like 2, 3 will be of more prominence as other uncertainties from flux, luminosities and detector systematics should be considered alongwith statistical error .

to that in the lower panel of Fig. 3. We see that without the effect of the distribution function almost all values of $\phi_{\nu_e}^r (= \phi_{\bar{\nu}_e}^r)$ would give hierarchy sensitivity to at least 1σ C.L., while for lower values of the relative luminosity the sensitivity can be seen to be rather good. As we increase σ the sensitivity is seen to go down for all value of the relative luminosity. We find that even for very small values of $\sigma = 0.05$, there is almost no hierarchy sensitivity for $\langle \phi_{\nu_e}^r \rangle (= \langle \phi_{\bar{\nu}_e}^r \rangle) \gtrsim 1$. As σ increases this pattern remains the same, though the sensitivity keeps falling for all values of $\langle \phi_{\nu_e}^r \rangle (= \langle \phi_{\bar{\nu}_e}^r \rangle)$. In the above analysis, σ is considered in a small range. The idea was to avoid deviating too much from the simulated values of the relative initial luminosities. If the actual variations of $\phi_{\nu_e}^r$ for all past supernovae are much larger than the range considered here, then the difference between predicted events for NH and IH would decrease even further, and this could washout the hierarchy sensitivity even for the low $\phi_{\nu_e}^r$ cases.

Finally in Fig. 5 we display how we can make sure quantitatively that the observed number of events belong to one of the hierarchies and not the other one and see its dependence on the exposure in Mton-Yr. Fig. 5 plots the ratio $\frac{|N_{NH} - N_{IH}|}{\sqrt{N_{NH} + N_{IH}}}$ for four different values of the exposure i.e. 2.5, 5.0, 7.5 and 10.0 Mton-Yr as a function of the expectation values of the relative flux, $\langle \phi_{\nu_e}^r \rangle$ taken as equal to $\langle \phi_{\bar{\nu}_e}^r \rangle$. This is for the case $P_H=1$ and with $\sigma=0.20$. This shows that with 2.5 Mton-Yr, the relative flux expectations with values below 0.95 (ratio ~ 1) can distinguish NH from IH (at least in principle) as the statistical error is smaller than the number of event difference. However to achieve a better

sensitivity i.e ratio ~ 2 the upper limit for the relative flux expectations is about 0.77. For ratio ~ 3 the value is even lower. However with larger values of exposures like 5.0 or 7.5 Mton-Yr one can still make a distinction between hierarchies when the centroid is below 0.75 and 0.82 respectively. But it is clear from the figure that by increasing the Mton-Yr one gets only a slow increase in the allowed parameter space.

IV. CONCLUSION

In this work we studied the prospects of measuring the neutrino mass hierarchy from observation of the DSNB signal in terrestrial detectors. While such studies have been performed before by different groups including ours, our work is unique as this is the first time that distribution of the source SN with initial relative neutrino and antineutrino fluxes has been taken into account. It is natural that different SN would emit neutrino and antineutrino fluxes with slightly different initial conditions, depending on the properties of the progenitor star. This is particularly relevant in the context of collective oscillations, where the multiple split patterns depend crucially on the initial relative fluxes. Since the actual distribution function of SN with the initial relative fluxes are unknown, we chose four specimen distribution functions, which have a mean corresponding to the value from SN simulations and a width such that almost all the values are within a factor of two of the mean value. We worked with three log-normal and one uniform distribution. We presented the DSNB fluxes for all the four distributions for both normal and inverted hierarchies. We calculated the total predicted number of $\bar{\nu}_e$ events in water detectors, both with and without Gadolinium. The log-normal distribution is characterized by its mean value and its variance. These are parametrized in terms of the variables μ and σ . We studied the dependence of the hierarchy sensitivity to the mean and variance of the log-normal distribution function. We concluded that the hierarchy sensitivity in this experiment had a crucial dependence on the mean value of the relative initial luminosity $\phi_{\nu_e}^r$ and $\phi_{\bar{\nu}_e}^r$. The sensitivity has a predominantly non-linear dependence on $\langle\phi_{\nu_e}^r\rangle$ and $\langle\phi_{\bar{\nu}_e}^r\rangle$, being higher for lower values of these quantities. The effect of the variance parametrized by σ is to reduce the hierarchy sensitivity for all values of the mean $\langle\phi_{\nu_e}^r\rangle$ and $\langle\phi_{\bar{\nu}_e}^r\rangle$. We

found that even for very moderate values of $\sigma \simeq 0.05$, there is almost no hierarchy sensitivity in the very small mixing angle limit for $\langle\phi_{\nu_e}^r\rangle = \langle\phi_{\bar{\nu}_e}^r\rangle \gtrsim 1$.

Finally we discuss the issue of using an effective two flavor evolution followed in this paper. As mentioned earlier if the analysis is done using all three flavors only the ‘double splits’ for IH arising in a small part of the $(\phi_{\nu_e}^r, \phi_{\bar{\nu}_e}^r)$ parameter space seen in the two flavor case change to ‘single split’ while things remain unchanged for NH. This effect would have been important for calculations for a single SN event if the initial flux ratios fell in this part of the parameter space. However for DSNB with averaging done over the SN distributions (D_i) the three flavor treatment will result in small corrections to the effective two flavor results presented here.

To summarize, using some reasonable simplifying assumptions we for the first time take into account, for calculating DSNB, a distribution in the relative fluxes in SN neutrinos and study its effect on the ability to distinguish the two hierarchies through a future observation of DSNB. A more detailed and rigorous study involving multi-angle effects and three flavors will be able to give more exhaustive answers to many of the aspects and should be pursued in future. But the model calculation carried out in this paper asserts that for DSNB which is a blend of many SN, not all identical, it is more difficult to distinguish IH from NH compared to a single SN or the hypothetical case of DSNB made of supernovae with identical flux ratios. A few favorable scenarios for this hierarchy distinguishability are indicated. We feel that the central finding of this first study is robust and will survive more detailed analysis

Acknowledgments

The authors would like to thank Basudeb Dasgupta for valuable comments and suggestions. S. Chakraborty acknowledges hospitality at Harish-Chandra Research Institute during the development stage of this work. S. Choubey acknowledges support from the Neutrino Project under the XI Plan of Harish-Chandra Research Institute. K. Kar and S. Chakraborty acknowledge support from the projects ‘Center for Astroparticle Physics’ and ‘Frontiers of Theoretical Physics’ of Saha Institute of Nuclear Physics.

-
- [1] R.M. Bionta et al., Phys. Rev. Lett. **58** 1494 (1987) .
 - [2] E.N. Alexeyev et al., JETP Lett. **45** 589.(1987)
 - [3] K.S. Hirata et al., Phys. Rev. Lett. **58** 1490.(1987)
 - [4] A. S. Dighe and A. Y. Smirnov, Phys. Rev. D **62** (2000) 033007 arXiv:hep-ph/9907423.
 - [5] C. Lunardini and A. Yu. Smirnov, JCAP **0306**, 009 (2003) arXiv:hep-ph/0302033.
 - [6] J. T. Pantaleone, Phys. Lett. B **287**, 128 (1992).
 - [7] G. Sigl and G. Raffelt, Nucl. Phys. B **406**, 423 (1993).
 - [8] V. A. Kostelecky and S. Samuel, Phys. Rev. D **52**, 621 (1995).
 - [9] S. Pastor, G. G. Raffelt and D. V. Semikoz, Phys. Rev. D **65**, 053011 (2002).
 - [10] Y. Y. Y. Wong, Phys. Rev. D **66**, 025015 (2002).
 - [11] A. B. Balantekin and Y. Pehlivan, J. Phys. G **34**, 47 (2007).

- [12] S. Pastor and G. Raffelt, Phys. Rev. Lett. **89**, 191101 (2002).
- [13] R. F. Sawyer, Phys. Rev. D **72**, 045003 (2005).
- [14] H. Duan, G. M. Fuller and Y. Z. Qian, Phys. Rev. D **74**, 123004 (2006).
- [15] H. Duan, G. M. Fuller, J. Carlson and Y. Z. Qian, Phys. Rev. D **74**, 105014 (2006).
- [16] S. Hannestad, G. G. Raffelt, G. Sigl and Y. Y. Y. Wong, Phys. Rev. D **74**, 105010 (2006); Erratum *ibid.* **76**, 029901 (2007).
- [17] G. G. Raffelt and G. Sigl, Phys. Rev. D **75**, 083002 (2007).
- [18] A. Esteban-Pretel *et al.*, Phys. Rev. D **76**, 125018 (2007).
- [19] H. Duan, G. M. Fuller, J. Carlson and Y. Z. Qian, Phys. Rev. D **75**, 125005 (2007).
- [20] G. G. Raffelt and A. Yu. Smirnov, Phys. Rev. D **76**, 081301 (2007); Erratum *ibid.* **77**, 029903 (2008).
- [21] G. G. Raffelt and A. Yu. Smirnov, Phys. Rev. D **76**, 125008 (2007).
- [22] H. Duan, G. M. Fuller and Y. Z. Qian, Phys. Rev. D **76**, 085013 (2007).
- [23] H. Duan, G. M. Fuller, J. Carlson and Y. Z. Qian, Phys. Rev. Lett. **99**, 241802 (2007).
- [24] G. L. Fogli, E. Lisi, A. Marrone and A. Mirizzi, JCAP **0712**, 010 (2007).
- [25] G. L. Fogli *et al.*, Phys. Rev. D **78**, 097301 (2008).
- [26] H. Duan, G. M. Fuller, J. Carlson and Y. Z. Qian, Phys. Rev. Lett. **100**, 021101 (2008).
- [27] B. Dasgupta, A. Dighe, A. Mirizzi and G. G. Raffelt, Phys. Rev. D **77**, 113007 (2008).
- [28] B. Dasgupta and A. Dighe, Phys. Rev. D **77**, 113002 (2008).
- [29] H. Duan, G. M. Fuller and Y. Z. Qian, Phys. Rev. D **77**, 085016 (2008).
- [30] B. Dasgupta, A. Dighe and A. Mirizzi, Phys. Rev. Lett. **101**, 171801 (2008).
- [31] A. Esteban-Pretel *et al.*, Phys. Rev. D **78**, 085012 (2008).
- [32] B. Dasgupta, A. Dighe, A. Mirizzi and G. G. Raffelt, Phys. Rev. D **78**, 033014 (2008) [arXiv:0805.3300].
- [33] J. Gava and C. Volpe, Phys. Rev. D **78**, 083007 (2008).
- [34] G. G. Raffelt, Phys. Rev. D **78**, 125015 (2008).
- [35] G. Fogli, E. Lisi, A. Marrone and I. Tamborra, JCAP **0904**, 030 (2009)
- [36] B. Dasgupta, A. Dighe, G. G. Raffelt and A. Y. Smirnov, Phys. Rev. Lett. **103**, 051105 (2009)
- [37] G. Fogli, E. Lisi, A. Marrone and I. Tamborra, arXiv:0907.5115 [hep-ph].
- [38] S. Chakraborty, S. Choubey, S. Goswami and K. Kar, JCAP **1006**, 007 (2010) [arXiv:0911.1218 [hep-ph]].
- [39] A. Friedland, Phys. Rev. Lett. **104**, 191102 (2010)
- [40] H. Duan, G. M. Fuller and Y. Z. Qian, arXiv:1001.2799 [hep-ph].
- [41] B. Dasgupta, G. G. Raffelt and I. Tamborra, Phys. Rev. D **81**, 073004 (2010) [arXiv:1001.5396 [hep-ph]].
- [42] B. Dasgupta *et al.* [arXiv:1002.2943 [hep-ph]]
- [43] G. G. Raffelt and I. Tamborra, arXiv:1006.0002 [hep-ph].
- [44] G. S. Bisnovatyi-Kogan and S. F. Seidov Annals N. Y. Acad. Sci. **422**, 319 (1984).
- [45] L. M. Krauss, S. L. Glashow and D. N. Schramm, Nature **310**, 191 (1984).
- [46] S. E. Woosley, J. R. Wilson and R. Mayle Astrophys. J. **302**, 19 (1986).
- [47] R. A. Malaney, Astropart. Phys. **7** 125 (1997)
- [48] D. H. Hartmann and S. E. Woosley, Astropart. Phys. **7** 137.(1997)
- [49] T. Totani, K. Sato and Y. Yoshii, Astrophys. J. **460** 303 (1996) arXiv:astro-ph/9509130.
- [50] M. Kaplinghat, G. Steigman and T. P. Walker, Phys. Rev. D **62** 043001 (2000) arXiv:astro-ph/9912391.
- [51] L. E. Strigari, M. Kaplinghat, G. Steigman and T. P. Walker, JCAP **0403** 007 (2004)
- [52] M. Fukugita and M. Kawasaki, Mon. Not. Roy. Astron. Soc. **340** L7 (2003) arXiv:astro-ph/0204376.
- [53] M. Wurm, F. von Feilitzsch, M. Goeger-Neff, K. A. Hochmuth, T. M. Undagoitia, L. Oberauer and W. Potzel, Phys. Rev. D **75** 023007 (2007)
- [54] S. Ando and K. Sato, New J. Phys. **6** 170 (2004)
- [55] E. Cappellaro, M. Turatto, D. Y. Tsvetkov, O. S. Bartunov, C. Pollas, R. Evans and M. Hamuy, Astron. Astrophys. **322** 431 (1997)
- [56] S. Ando, K. Sato and T. Totani, Astropart. Phys. **18** 307 (2003)
- [57] S. Ando and K. Sato, Phys. Lett. B **559** 113 (2003)
- [58] C. Lunardini, Astropart. Phys. **26** 190 (2006)
- [59] S. Ando, Astrophys. J. **607** 20 (2004)
- [60] C. Volpe and J. Welzel, arXiv:0711.3237 [astro-ph].
- [61] A. G. Cocco, A. Ereditato, G. Fiorillo, G. Mangano and V. Pettorino, JCAP **0412**, 002 (2004)
- [62] L. E. Strigari, J. F. Beacom, T. P. Walker and P. Zhang, JCAP **0504**, 017 (2005)
- [63] J. F. Beacom and L. E. Strigari, Phys. Rev. C **73** 035807 (2006)
- [64] C. Lunardini, Phys. Rev. D **73** 083009 (2006)
- [65] S. Chakraborty, S. Choubey, B. Dasgupta and K. Kar, JCAP **0809**, 013 (2008)
- [66] S. Galais, J. Kneller, C. Volpe and J. Gava, Phys. Rev. D **81**, 053002 (2010)
- [67] M. Malek *et al.* [Super-Kamiokande Collaboration], Phys. Rev. Lett. **90** 061101 (2003)
- [68] M. Aglietta *et al.*, Astropart. Phys. **1** 1 (1992)
- [69] A.M. Hopkins and J.F. Beacom, Astrophys. J. **651**, 142 (2006).
- [70] M.D. Kistler et al, arXiv:0709.0381v2 [astro-ph].
- [71] C. Amsler *et al.* [Particle Data Group], "Review of particle physics," Phys. Lett. B **667**, 1 (2008).
- [72] I.K. Baldry and K. Glazebrook, Astrophys. J. **593**, 258 (2003).
- [73] P. Bhattacharjee, S. Chakraborty, S. Das Gupta, K. Kar, Phys. Rev. D **77**, 043008 (2008)
- [74] Madau P, Pozzetti L and Dickinson M *Astrophys. J.* **498** 106 1998
- [75] M. T. Keil, G. G. Raffelt and H. T. Janka, Astrophys. J. **590** 971 (2003)
- [76] R. Tomas, M. Kachelriess, G. Raffelt, A. Dighe, H. T. Janka and L. Scheck, JCAP **0409**, 015 (2004)
- [77] R. C. Schirato and G. M. Fuller, arXiv:astro-ph/0205390.
- [78] H. Duan and A. Friedland, Phys. Rev. Lett. **106**, 091101 (2011)
- [79] A. Bandyopadhyay et al, arXiv:hep-ph/0312315.
- [80] M. T. Keil, arXiv:astro-ph/0308228.
- [81] Y. Itow *et al.*, arXiv:hep-ex/0106019.
- [82] A. de Bellefon *et al.*, arXiv:hep-ex/0607026.
- [83] C. K. Jung, AIP Conf. Proc. **533**, 29 (2000).
- [84] J. F. Beacom and M. R. Vagins, Phys. Rev. Lett. **93**, 171101 (2004)
- [85] A. Rubbia, arXiv:hep-ph/0402110;
- [86] www-off-axis.fnal.gov/flare/
- [87] B. Baibussinov *et al.*, Astropart. Phys. **29**, 174 (2008)